STATE RESEARCH CENTER OF RUSSIA
INSTITUTE FOR HIGH ENERGY PHYSICS

IHEP 2012-25

O.V. Stenyakin, O.P. Yushchenko

The LHCb ECAL and Preshower calibration with isolated electrons

Protvino 2012

UDK 519.25.256 M–24

Abstract

Stenyakin O.V., Yushchenko O.P. The LHCb ECAL and Preshower calibration with isolated electrons: IHEP Preprint 2012-25. – Protvino, 2012. – p. 18, figs. 10, tables 3, refs.: 8.

The results of the calibration of the LHCb electromagnetic calorimeter ECAL and Preshower detector on the real data recorded in 2010, 2011 and 2012 are presented. The calibration procedure and track selection requirements are described. The implemented calibration method is very fast and allows to perform the ECAL and Preshower calibration simultaneously.

Аннотация

Стенякин О.В., Ющенко О.П. Калибровка электромагнитного калориметра ECAL и предливневого детектора Preshower эксперимента LHCb с помощью изолированных электронов: Препринт ИФВЭ 2012-25. – Протвино, 2012. – 18 с., 10 рис., 3 табл., библиогр.: 8.

В работе представлены результаты калибровки электромагнитного калориметра ECAL и предливневого детектора Preshower эксперимента LHCb с помощью изолированных электронов, полученных из реальных данных в 2010, 2011 и 2012 гг. Приведено описание процедуры калибровки и необходимого для её выполнения метода отбора треков. Данный метод калибровки отличается высокой скоростью и позволяет проводить калибровку калориметра ECAL и детектора Preshower одновременно.

Introduction

A precise calibration of the electromagnetic calorimeter is a key task in any high energy physics experiment. This calibration should allow a correct reconstruction of electromagnetic shower energies.

It is well known that the calibration can be performed with an electron beam of fixed energy. The methods based on comparison of reconstructed π^0 mass with true one are also used [1].

Another interesting possibility consists in a usage of electrons/positrons produced in real events. The main idea consists in the identification of electrons without usage of the ECAL (by RICH, for example), measurement of their momenta by tracking system and comparison of the energy deposition in the ECAL with measured momentum.

In this case we do not care about sources of electrons. In particular, in the case of the LHCb experiment they can be produced in B- and D-mesons semileptonic inclusive decays as well as due to photons conversion in material of VELO detector and other upstream detector elements [2].

In this note we present selection procedures, the method of calibration coefficient calculations and final correction factors to be used in the ECAL and Preshower calibration with the data samples collected by the LHCb detector in 2010, 2011 and 2012.

The calorimeter system of the LHCb experiment is described in Sec. 1. The problem definition to determine the calibration coefficients is described in Sec. 2. The details of the electron selections and data samples used for the calibration are described in Sec. 3. The calibration procedure and the correction factors to the energy deposition of the calorimeters are described in Sec. 4. In Sec. 5 results of the calibration and time stability of the electromagnetic calorimeter and Preshower detector are presented.

1. The LHCb calorimeter system

The calorimeter system [3, 4, 5, 6, 7] is composed of the Scintillator Pad Detector and Preshower Detector (SPD/PS), an electromagnetic ("shashlik" type) calorimeter (ECAL) and a hadronic (`Fe` and scintillator tiles) calorimeter (HCAL). The thickness of the ECAL is chosen to be 25 radiation lengths to provide complete shower absorption in the energy range of the detector. Due to the strong variation of the secondary particles flow over the calorimeter surface, three sections with different transverse cell size are used in the SPD/PS and ECAL. Each of the SPD, PS and ECAL detectors has 6016 channels. The Fig. 1 shows the details of the calorimeters structure.

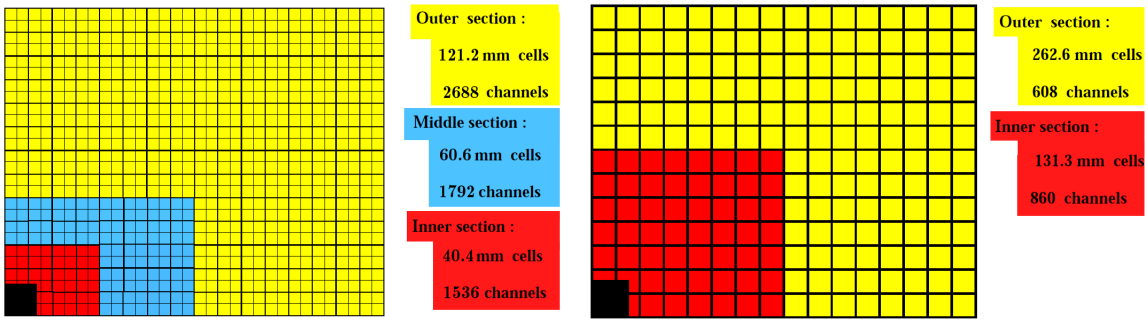

Figure 1. Lateral segmentation of the SPD/PS and ECAL (left) and the HCAL (right). One quarter of the detector front face is shown. In the left figure the cells dimensions are given for ECAL. For SPD/PS they should be reduce by $\approx 1.5\%$.

2. Problem definition

In original formulation the problem consists in the determination of the calibration coefficients for the calculation of energy deposition in the electromagnetic calorimeter and Preshower detector based on data from recorded ADC values.

In general, this can be done starting from the RAW (not reconstructed) data where original ADC counts are presented. This implies also electrons identification, pattern recognition in the tracking system and momentum reconstruction and can be done in separate reconstruction stream. Nevertheless, the task can be significantly simplified if one will relay on the DSTs with complete ID and tracking procedures performed in the standard reconstruction stream.

The DST (Data Summary "Tape") is the format used to store the reconstructed LHCb data. The DST data contain cells energy deposition for the ECAL and PS obtained with the dedicated calibration procedure which uses different corrections and calibration methods. Using data presented in DST which are essentially energy depositions we will provide additional multiplicative corrections obtained with method described in this note.

The Preshower detector (in which an electromagnetic shower starts) is located in front of the ECAL. Therefore the total energy deposition of electron/photon should be considered as a linear combination of energy depositions in the ECAL and Preshower.

3. Data samples and selections

As mentioned above all the analysis is based on the DSTs where ID and track information as well as calibrated energy deposition are given. The tracks ID information on the DST provides a possibility to perform RICH-based ID as well as combined identification based on RICH and calorimeters and muon system information. To make a selection of the electron we use the variable `bestParticleID` which is based on RICH information only. It is chosen on the basis of a combined DLL value (Delta Log Likelihood) which is calculated with respect to charged π-meson (DLL of $\pi^{\pm}$ is assumed to be 0). We could make better selection of the electrons by making a stronger cut on DLL value. But this method does not lead to a noticeable improvement and significantly reduces the final statistics. So, finally, we rely on the standard RICH-based electron identification.

In order to ensure the purity of the data sample only isolated tracks are used. That means that there is no other track in some neighbourhood at the ECAL entrance. We choose this one as a circle with 30 cm radius to avoid overlap of showers in the ECAL. The selected size of the circle is sufficient to cover a shower in 3×3 cluster in each zone of the ECAL.

For the same reason we use tracks with large momentum value. For 2010 data there are electrons with momentum $p_e > 10$ GeV/c and for 2011 and 2012 — with $p_e > 3$ GeV/c. As a result, the data sample is sufficiently clean without significant hadronic contribution (see Fig. 2 as an example).

So we want to calibrate the Preshower as well we select electromagnetic showers which start in the PS by the requirement $E_{tot}(PS) > 20$ MeV for PS 3×3 cluster associated with the track. On the other hand, to reduce a background from hadrons we should limit the energy deposition in the HCAL cluster. It is set to $E_{tot}(HCAL) < 1$ GeV.

The final selection requirements are shown in the following list:

- Only RICH is used to identify electrons;
- Track momentum $p_e > 10$ GeV/c (2010) or $p_e > 3$ GeV/c (2011, 2012);
- Only isolated electrons are used: no other charged tracks within the circle with $R = 30$ cm at ECAL entrance;
- Total Preshower energy deposition associated with the track $E_{tot}(PS) > 20$ MeV;
- Total HCAL energy deposition associated with the track $E_{tot}(HCAL) < 1$ GeV.

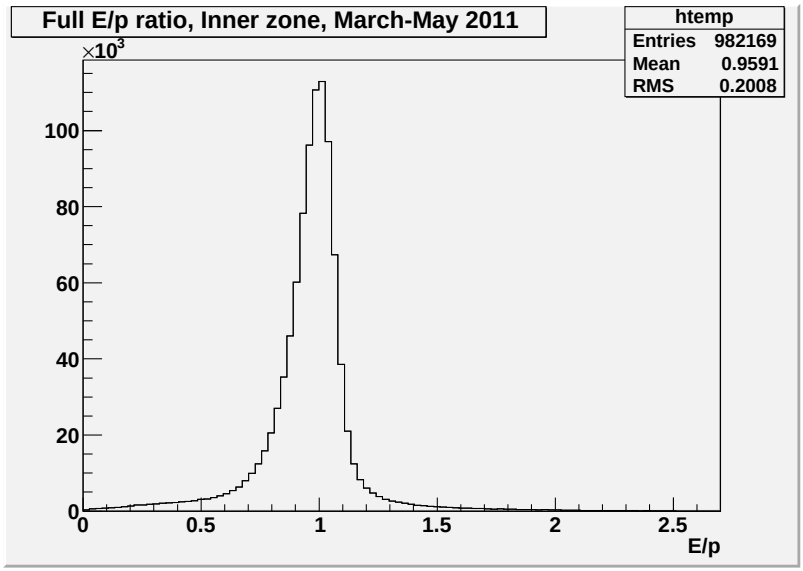

Figure 2. The E/p ratio for inner zone of the ECAL and PS for March—May 2011 data.

3.1. 2010 dataset

As mentioned before we use the real data for calibration which are essentially the standard reconstruction streams, i.e. for our calibration procedure we do not require special reconstruction procedures. For 2010 calibration we use the latest LHCb data reconstruction (`Reco05`, `Stripping09`).

Several DSTs are considered to search for electrons satisfying the requirements of the selections. In Table 1 the approximate number of total events and e-candidates we obtain in the different DSTs are shown. The HADRONIC.DST and MINIBIAS.DST are selected due to the greatest number of the required e-candidates. They contain about 1.50×10^8 and 0.42×10^8 e-candidates respectively. In total about 4.00×10^8 physical events collected by the LHCb experiment in 2010 were processed and about 8.00×10^6 electrons were selected.

Table 1. The approximate number of total events and e-candidates in DSTs of 2010. All values are in 10^6 events.

Data stream	MagDown	MagUp	N_{tot}	N_e	N_e/N_{tot}
HADRONIC.DST	197.0	112.8	309.8	149.6	48.3%
MINIBIAS.DST	93.5	79.5	173.0	42.3	25%
EW.DST	29.0	12.8	41.8	18.9	45%
SEMILEPTONIC.DST	17.0	6.6	23.6	11.0	47%
DIELECTRON.DST	14.3	6.3	20.6	10.7	52%

To select and collect the information about required electrons the selection algorithm was written and it was executed by the LHCb physics analysis software `DaVinci v26r0`.

3.2. 2011 dataset

For 2011 calibration the `Reco12`, `Stripping17` reconstruction streams for the data and `DaVinci v29r1` are used. The BHADRON.DST and EW.DST were selected to perform the calibration (see Table 2 for details). In total about 4.80×10^8 physical events collected by the LHCb were processed and about 1.56×10^8 e-candidates were selected.

Table 2. The approximate number of total events and e-candidates by DSTs in 2011. All values are in 10^6 events.

Data stream	MagDown	MagUp	N_{tot}	N_e	N_e/N_{tot}
BHADRON.DST	169.0	114.8	283.8	105.0	37%
EW.DST	114.7	83.5	198.2	51.5	26%

In 2011 we were able to perform several new tasks:

- full Preshower calibration,
- study of the time stability of the ECAL.

These studies were not performed previously due to the small statistics which became much higher in 2011 and 2012.

3.3. 2012 dataset

For 2012 calibration the `Reco14`, `Stripping20` reconstruction streams for the data and `DaVinci v31r0` are used. The EW.DST and BHADRONCOMPLETEEVENT.DST were selected to perform the calibration. In total about 8.00×10^8 physical events collected by the LHCb were processed and about 1.25×10^8 e-candidates were selected.

In this case as an initial one we used the calibration from the LHCb Conditions Database [8] with tag `cond-20120929`. It is valid for following periods of data taking (until 29th of August 2012) and for corresponding first and last run numbers:

1. April, 111181—113146;
2. May, 114205—117103;
3. June, 117192—118880;
4. July, 119560—124308;
5. August, 124333—126339.

For data taking in September 2012 (corresponding first and last run numbers: 126972—129644) we used the Conditions Database tag `cond-20121116`.

4. The calibration procedure

The calibration algorithm starts from the determination of the track entry point in the calorimeter. Then we consider the closest 3×3 ECAL cluster around the cell which is pointed out by the track. Then we build the E/p ratio where E is a sum of total energy depositions in the ECAL and PS clusters and p is the track momentum measured by the tracking system. We assume that the E/p ratio should be equal to unity in the ideally calibrated calorimeter:

$$\frac{E}{p} \equiv \frac{E_{tot}(ECAL) + E_{tot}(PS)}{p} \simeq 1. \tag{1}$$

A consideration of the PS energy is performed in two ways. First, we assume the total PS energy deposition is a sum of cells energy in PS cluster with weight factor α:

$$E_{tot}(PS) = \alpha \sum_{cells} E_l^{PS}. \tag{2}$$

In general, the α value depends on the zone of calorimeter and therefore we calculate α-factors for each zone of the ECAL (or PS) separately. So, α-factors are individual for each zone. The calibration was performed this way for 2010 data (see Sec. 4.1). For 2011 and 2012 data (see Sec. 4.2) we performed calibration of the Preshower and calculated the α-factors for each cell of the Preshower. Then the total energy deposition in PS cluster is given by:

$$E_{tot}(PS) = \sum_{cells} \alpha_l E_l^{PS}. \tag{3}$$

In both cases the calibration is performed for each zone of the ECAL and PS separately. The weight factors α are considered to be the parameters in the minimization procedure which is described below.

To avoid strong background contribution for small values of E/p the calibration coefficients for 2010 data are calculated for events with E/p values within the interval $E/p \in [0.8, 1.2]$ for inner and middle zones and within the interval $E/p \in [0.9, 1.1]$ for outer zone. For 2011 and 2012 data they are calculated for E/p values within the interval $E/p \in [0.8, 1.2]$ for all zones of the ECAL.

4.1. The ECAL calibration and contribution of the PS (2010)

The calibration coefficients are obtained by minimization of the following functional:

$$\chi^2(\alpha, \vec{C}) = \sum_{i=1}^{N} \frac{\left(\sum_{j=1}^{M} C_j E_{ij} + \alpha \sum_{l=1}^{L} E_{il}^{PS} - p_i \right)^2}{\sigma_i^2}, \tag{4}$$

where N — total number of tracks (e-candidates), M — number of cells in the ECAL cluster from i-th track, C_j — j-th element of the vector $\vec{C}$ of the ECAL calibration coefficients, E_{ij} — energy deposition in j-th cell of the ECAL cluster from i-th track, L — number of cells in the PS cluster from i-th track, α — weight factor for the PS energy deposition (individual for each zone), E_{il}^{PS} — energy deposition in l-th cell of the PS cluster from i-th track, p_i — momentum of i-th track, σ_i — energy resolution of the ECAL for i-th track. We took σ as:

$$\frac{\sigma_E}{E} = \frac{10\%}{\sqrt{E}} \oplus 1\% \qquad (E \text{ in GeV}). \tag{5}$$

We could expect that the multiplicative calibration coefficients should be close to 1 because ECAL as well as PS are already calibrated.

For simplicity we do not consider the variation of the values of σ due to the change of calibration coefficients during the fit procedure. This assumption could be considered as a good approximation in the case of small variation of final calibration coefficients with respect to unity. In the next section we will show that the variation of the obtained multiplicative corrections is within 3—5% only and we can consider the above approximation as good.

With this approximation the expression (4) is completely quadratic with respect to unknown coefficients. In this case the solution of the problem can be performed straightforward by considering first derivatives of the (4).

Calculation of the derivatives of χ^2 leads to the system of linear equations for calibration coefficients and α of the current zone:

$$\frac{\partial \chi^2}{\partial C_q}: \qquad \sum_{i=1}^{N} \frac{E_{iq} \cdot \left(\sum\limits_{j=1}^{M} C_j E_{ij} + \alpha E_i^{PS} \right)}{\sigma_i^2} = \sum_{i=1}^{N} \frac{p_i E_{iq}}{\sigma_i^2}, \tag{6}$$

$$\frac{\partial \chi^2}{\partial \alpha}: \qquad \sum_{i=1}^{N} \frac{E_i^{PS} \cdot \left(\sum\limits_{j=1}^{M} C_j E_{ij} + \alpha E_i^{PS} \right)}{\sigma_i^2} = \sum_{i=1}^{N} \frac{p_i E_i^{PS}}{\sigma_i^2}, \tag{7}$$

where $E_i^{PS} = \sum\limits_{l=1}^{L} E_{il}^{PS}$ and $q = 1, 2, ..., N_{cells}$. N_{cells} — a number of cells in current zone of the ECAL.

So, we have a system of $(N_{cells} + 1)$ equations for each zone of the ECAL and the appropriate solution will provide us with the required coefficients.

4.2. Simultaneous calibration of the ECAL and PS (2011, 2012)

The calibration coefficients are obtained by minimization of the following functional:

$$\chi^2(\vec{\alpha}, \vec{C}) = \sum_{i=1}^{N} \frac{\left(\sum\limits_{j=1}^{M} C_j E_{ij} + \sum\limits_{l=1}^{L} \alpha_l E_{il}^{PS} - p_i \right)^2}{\sigma_i^2}, \tag{8}$$

where $\vec{\alpha}$ — vector of weight factors for each cell of the PS.

Calculation the derivatives of χ^2 leads to the system of linear equations:

$$\frac{\partial \chi^2}{\partial C_q}: \qquad \sum_{i=1}^{N} \frac{E_{iq} \cdot \left(\sum\limits_{j=1}^{M} C_j E_{ij} + \sum\limits_{l=1}^{L} \alpha_l E_{il}^{PS} \right)}{\sigma_i^2} = \sum_{i=1}^{N} \frac{p_i E_{iq}}{\sigma_i^2}, \tag{9}$$

$$\frac{\partial \chi^2}{\partial \alpha_r}: \qquad \sum_{i=1}^{N} \frac{E_{ir}^{PS} \cdot \left(\sum\limits_{j=1}^{M} C_j E_{ij} + \sum\limits_{l=1}^{L} \alpha_l E_{il}^{PS} \right)}{\sigma_i^2} = \sum_{i=1}^{N} \frac{p_i E_{ir}^{PS}}{\sigma_i^2}, \tag{10}$$

$q = 1, 2, ..., N_{cells}^{ECAL}$ and $r = 1, 2, ..., N_{cells}^{PS}$. Usually $N_{cells}^{ECAL} = N_{cells}^{PS} \equiv N_{cells}$ and we should solve the system with $2N_{cells}$ equations.

It should be noticed that in outer zone for 2010—2012 calibration periods we had very small statistics in 56-th and 57-th rows in the ECAL. And therefore we excluded these rows of cells (and in ECAL, and in PS) from the minimization procedure. Thus, instead of 2688 cells in outer zone we computed coefficients just for 2560 cells.

5. Results

5.1. E/p results

After the minimization procedure with the full 2010 statistics we observed a visible improvement of the E/p ratios using the new coefficients compared with the old ones. For inner zone the value of this improvement is estimated at ∼17%, for middle zone — at ∼18% and for outer zone — at ∼20%. In Figs. 3 the E/p ratios with default coefficients (solid lines) and after fitting (dotted lines) for each zone of the ECAL are shown. To plot the histograms of the ECAL calibration coefficients (see also Figs. 3) we arrange them in ascending order by the columns and rows of the ECAL cells. We get a narrow

slightly biased peaks. The bias can be explained by the difference between the photon and electron shower development in the ECAL.

In the Table 3 the obtained values of α after fitting for each zone of the ECAL are shown.

Table 3. The table of α values after minimization for each zone of the ECAL (2010).

Zone of the ECAL	α value
Inner zone	15.645
Middle zone	12.96
Outer zone	9.68

In order to estimate the time stability of the ECAL and PS, the calibration for 2011 and 2012 data can be performed for each month of data taking. In Figs. 4—10 the E/p ratios, calibration coefficients of the ECAL and PS (α values), their mean and RMS values for each zone are shown[1]. In E/p figures we also see significant improvement in E/p peak widths. For inner zone this value is estimated to be $\sim$34%, $\sim$21% for middle zone and $\sim$12% for outer one in 2011. In 2012 for inner and middle zones we estimate improvement in E/p peak widths as about $\sim$25—40% and for outer zone as about $\sim$15%.

Errors of the ECAL calibration coefficients were also studied. Their typical values for 2011 and 2012 statistics are about 10^{-4}.

5.2. Time variations

Since the calibration for 2011 and 2012 data is performed by months it is possible to observe changes of the ECAL and PS coefficients throughout the year. In Figs. 5—10 mean and RMS values of calibration coefficients of the ECAL and PS by zones are shown. Each point at the figures corresponds to the processed dataset in current month. We see the increase of RMS values for all ECAL zones from March to October in 2011 (see Figs. 5, 7, 9). This proves the fact that the resolution of the calorimeter becomes worse to the end of the 2011. The same picture we observe for RMS values of the PS calibration coefficients in 2011 and 2012 (see Figs. 6, 8, 10).

The same study of time stability could not be implemented in 2010 due to small statistics.

[1] E/p ratios and distributions of coefficients only with March, April, May 2011 and April 2012 statistics are shown. Distributions for the rest periods are the same.

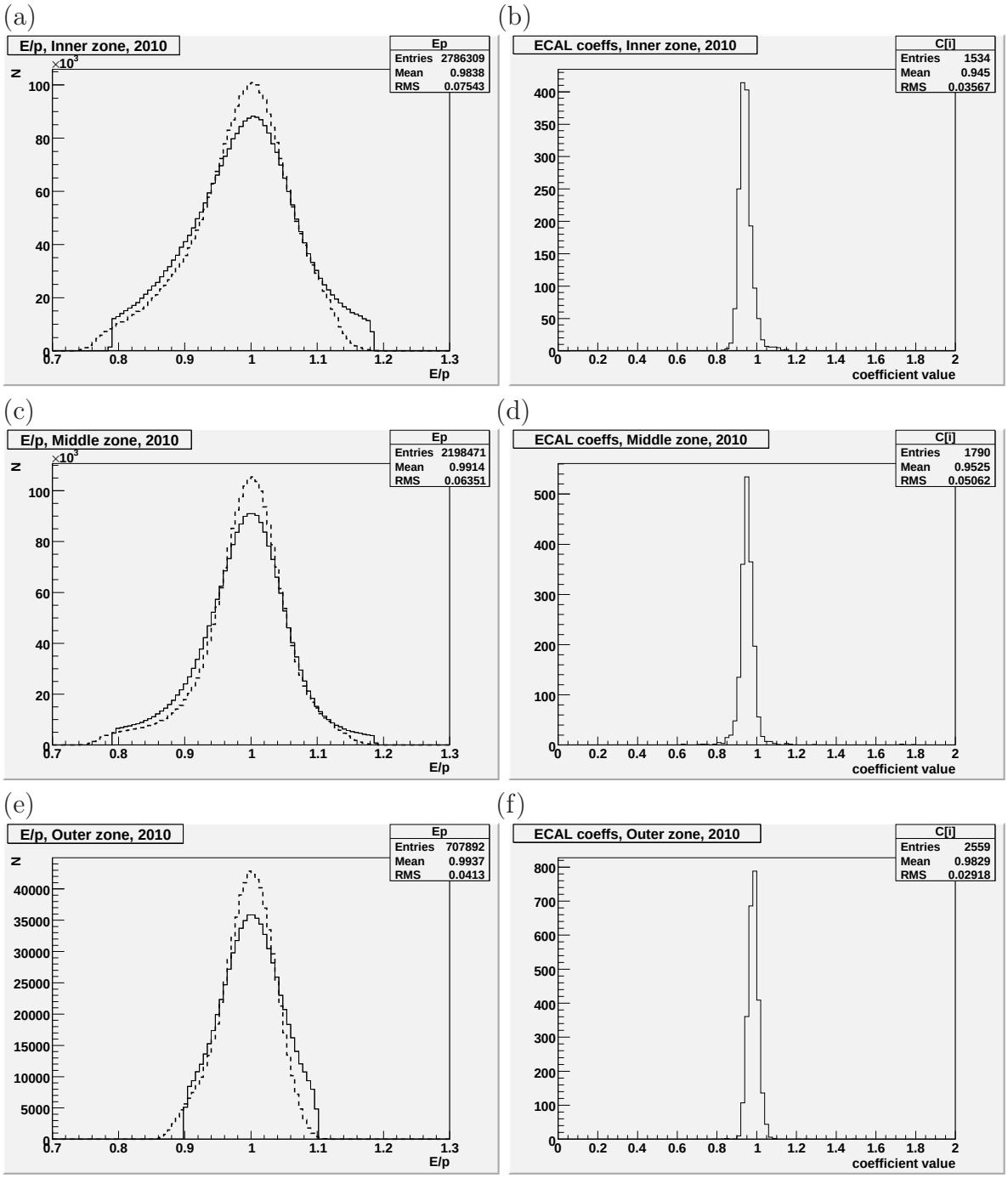

Figure 3. Selected intervals of the $E_{cluster}/p_{track}$ ratio with default coefficients (1.) (solid lines) and after fitting (dotted lines) and the ECAL calibration coefficients at 2010 statistics. (a), (b) for inner zone, (c), (d) for middle zone, (e), (f) for outer zone of the ECAL.

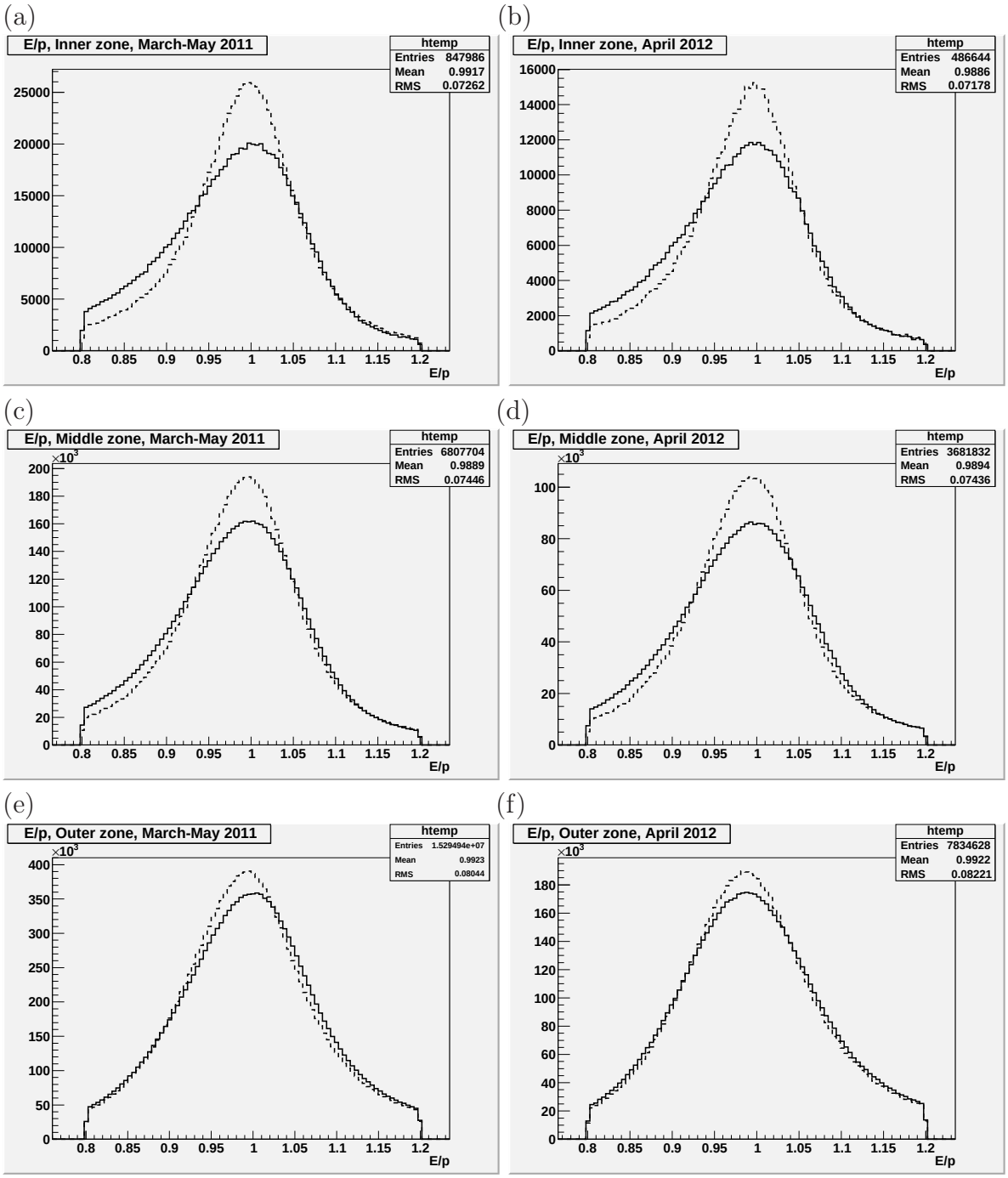

Figure 4. Selected intervals of the $E_{cluster}/p_{track}$ ratio with default coefficients (1.) (solid lines) and after fitting (dotted lines) for all zones of the ECAL. (a), (c), (e) March, April, May 2011 statistics and (b), (d), (f) April 2012 statistics.

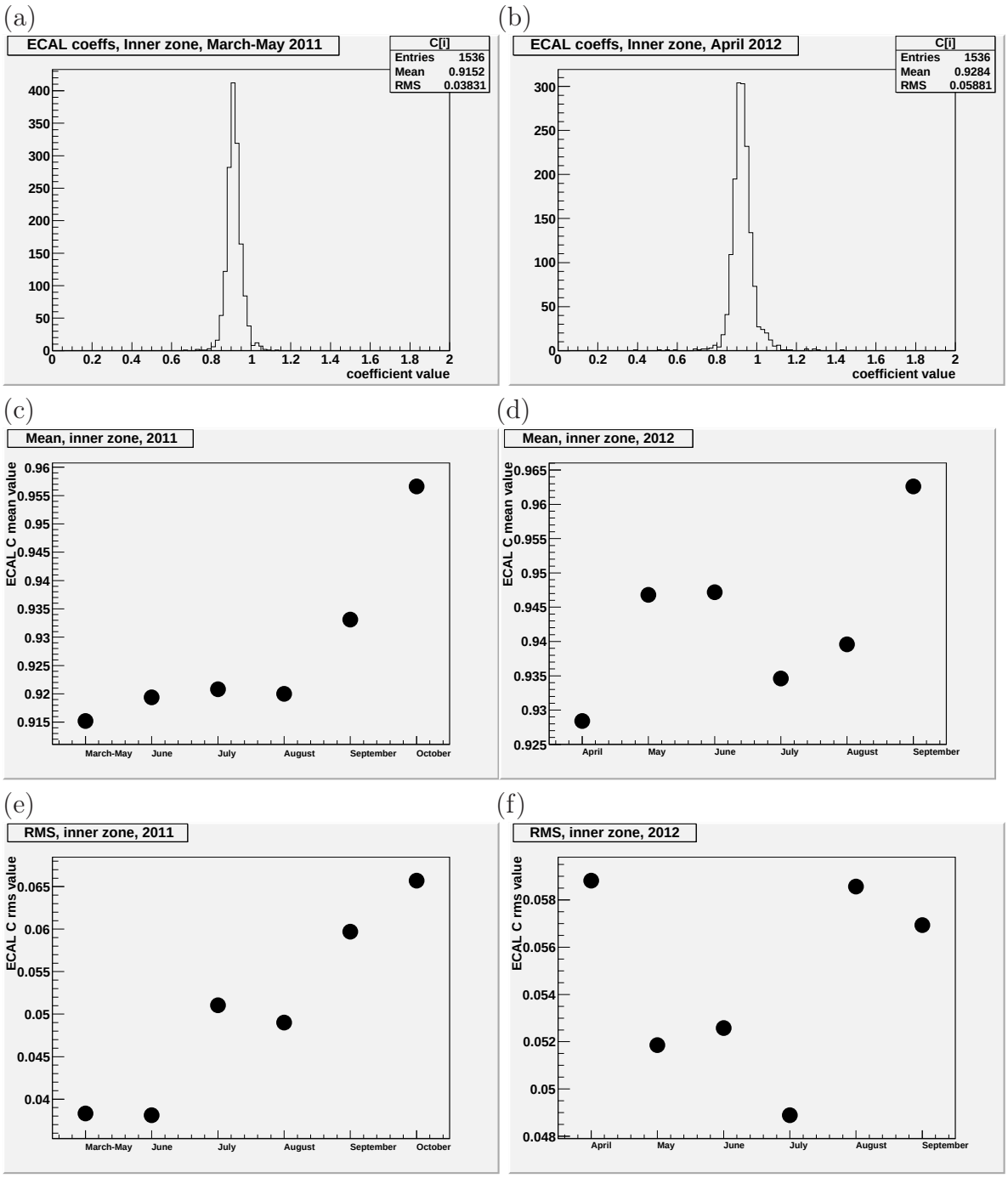

Figure 5. Distributions of calibration coefficients of the ECAL for inner zone: (a) March, April, May 2011 statistics, (b) April 2012 statistics. (c)—(f) Means and RMS values of calibration coefficients of the ECAL (inner zone) for different datasets.

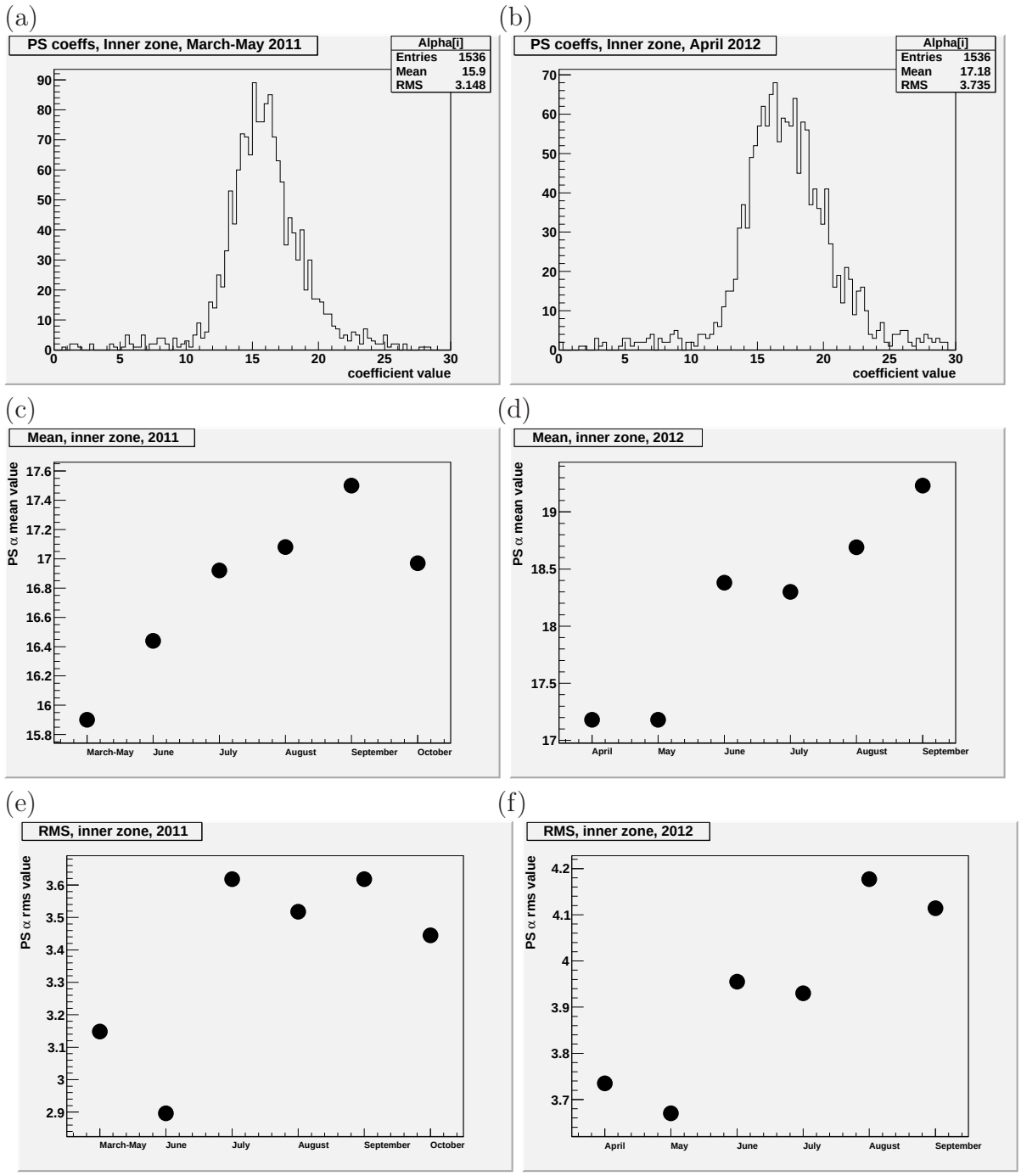

Figure 6. Distributions of calibration coefficients of the Preshower (α values) for inner zone: (a) March, April, May 2011 statistics, (b) April 2012 statistics. (c)—(f) Means and RMS values of calibration coefficients of the PS (inner zone) for different datasets.

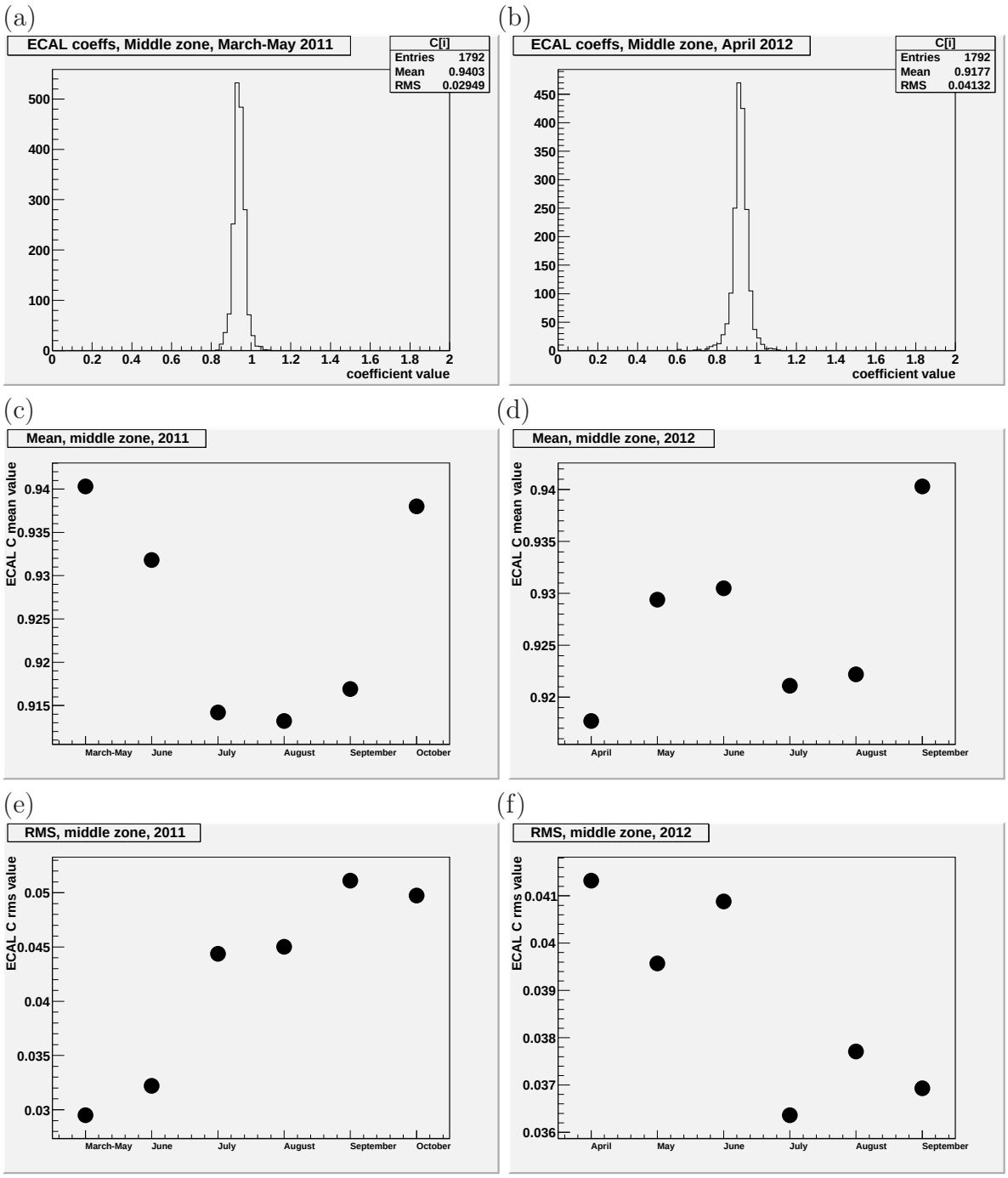

Figure 7. Distributions of calibration coefficients of the ECAL for middle zone: (a) March, April, May 2011 statistics, (b) April 2012 statistics. (c)—(f) Means and RMS values of calibration coefficients of the ECAL (middle zone) for different datasets.

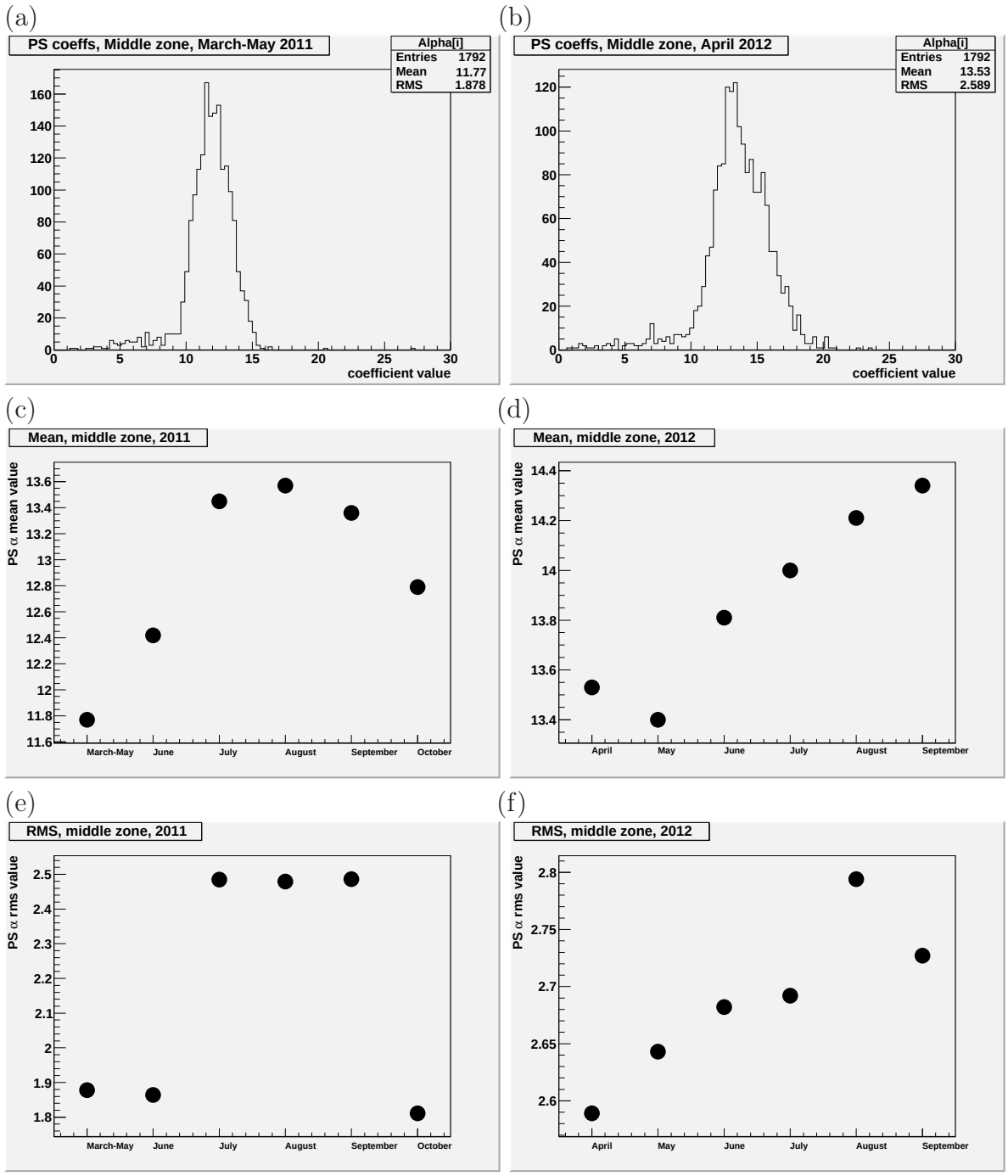

Figure 8. Distributions of calibration coefficients of the Preshower (α values) for middle zone: (a) March, April, May 2011 statistics, (b) April 2012 statistics. (c)—(f) Means and RMS values of calibration coefficients of the PS (middle zone) for different datasets.

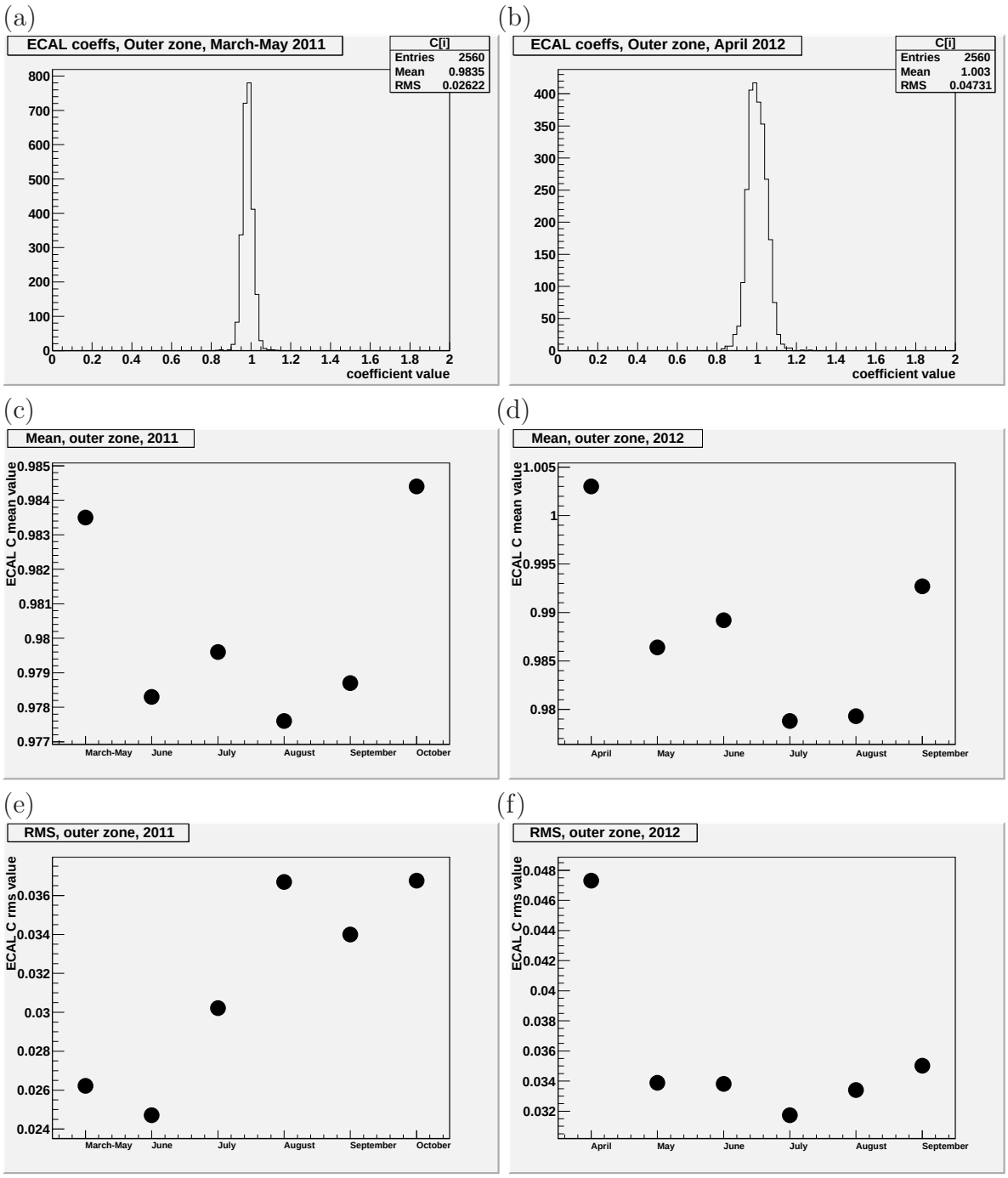

Figure 9. Distributions of calibration coefficients of the ECAL for outer zone: (a) March, April, May 2011 statistics, (b) April 2012 statistics. (c)—(f) Means and RMS values of calibration coefficients of the ECAL (outer zone) for different datasets.

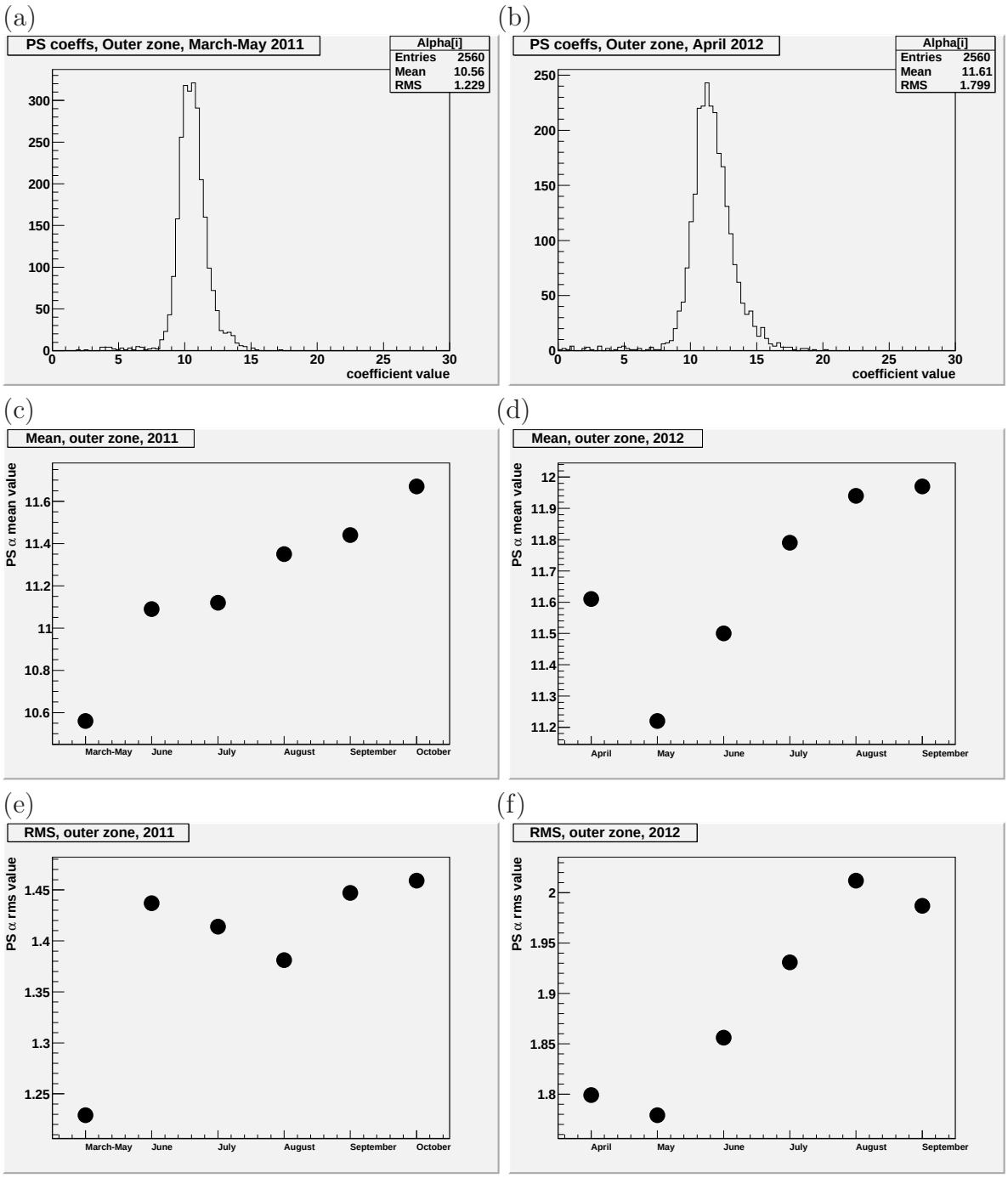

Figure 10. Distributions of calibration coefficients of the Preshower (α values) for outer zone: (a) March, April, May 2011 statistics, (b) April 2012 statistics. (c)—(f) Means and RMS values of calibration coefficients of the PS (outer zone) for different datasets.

6. Conclusion

In this note the results of the ECAL and Preshower calibration of the LHCb detector with isolated electrons obtained from the real data are shown. The calibration procedure and track selection requirements for that one are described.

The above calibration method is very fast and straightforward. It can be used to perform the ECAL and PS calibration simultaneously. In addition, we observe obvious time dependence of the ECAL and PS calibration coefficients. This proves the importance of the periodic precise calibration of the calorimeter system. Our studies show that the collected data sets are quite sufficient to fulfil this task without dedicated calibration runs.

Analysis of the complete 2010, 2011 and 2012 data sets result in the tables of the ECAL and PS multiplicative calibration coefficients which can be used for fine tuning of the calorimeter calibration. For 2011 and 2012 data time dependence of the calibration is also obtained. These results can be used to correct detector response variation with time.

The proposed calibration procedure results in visible improvement of E/p ratio. Nevertheless, the crucial test consists in the implementation of new calibration coefficients to π^0 reconstruction. This work is in progress now.

References

[1] A. Puig, D. Savrina, R. Graciani and I. Belyaev, *Kali: The framework for fine calibration of LHCb Electromagnetic Calorimeter*, LHCb-PROC-2011-027.

[2] I. Korolko, V.F. Obraztsov, S. Popescu and O.P. Yushchenko, *On the possibility of in situ calibration of LHCb calorimeters*, LHCb-2000-051.

[3] The LHCb Collaboration, *LHCb: Technical Proposal*, CERN-LHCC-98-004.

[4] The LHCb Collaboration, *LHCb reoptimized detector design and performance: TDR*, CERN-LHCC-2003-030.

[5] The LHCb Collaboration, *LHCb calorimeters: TDR*, CERN-LHCC-2000-036.

[6] The LHCb Collaboration, *The LHCb Detector at the LHC*, JINST **3** (2008) S08005.

[7] S. Barsuk *et al.*, *Design and construction of electromagnetic calorimeter for LHCb experiment*, LHCb-2000-043.

[8] M. Clemencic, N. Gilardi, J. Palacios, *LHCb Conditions Database*, LHCb-2006-017.

Received December 24, 2012.

Препринт отпечатан с оригинала-макета, подготовленного авторами.

О.В. Стенякин, О.П. Ющенко
Калибровка электромагнитного калориметра ECAL и предливневого детектора Preshower эксперимента LHCb с помощью изолированных электронов.

Оригинал-макет подготовлен с помощью системы **LaTeX.**

Подписано к печати 26.12.2012. Формат $60 \times 84/16$. Цифровая печать.
Печ.л. 1,38. Уч.-изд.л. 1,92. Тираж 80. Заказ 63. Индекс 3649.

ФГБУ ГНЦ ИФВЭ
142281, Протвино Московской обл.

Индекс 3649

П Р Е П Р И Н Т 2012–25, И Ф В Э, 2012